Image credit: NASA

Subhalo effective density slopes from HST strong lensing data with neural likelihood-ratio estimation

Gemma Zhang
Harvard University

CCA/IAP ML Workshop
November 2023

Zhang, Mishra-Sharma, Dvorkin, MNRAS (2208.13796)
Zhang, Şengül, Dvorkin, MNRAS (2308.09739)

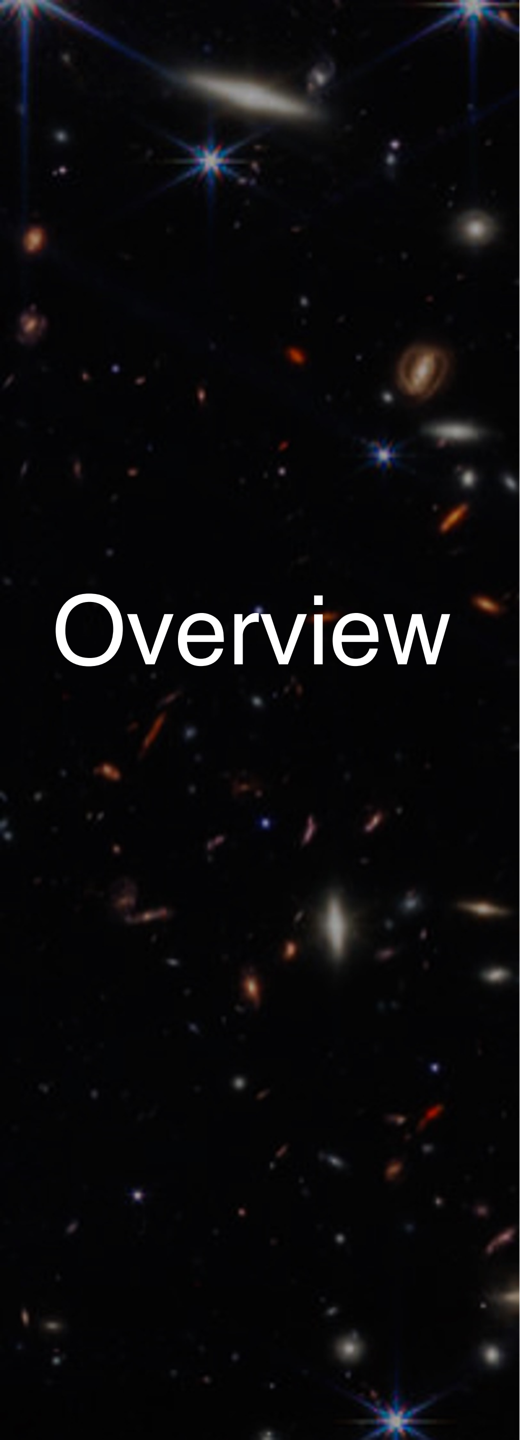

Overview

- Substructure in strong lensing
- Neural likelihood-ratio estimation

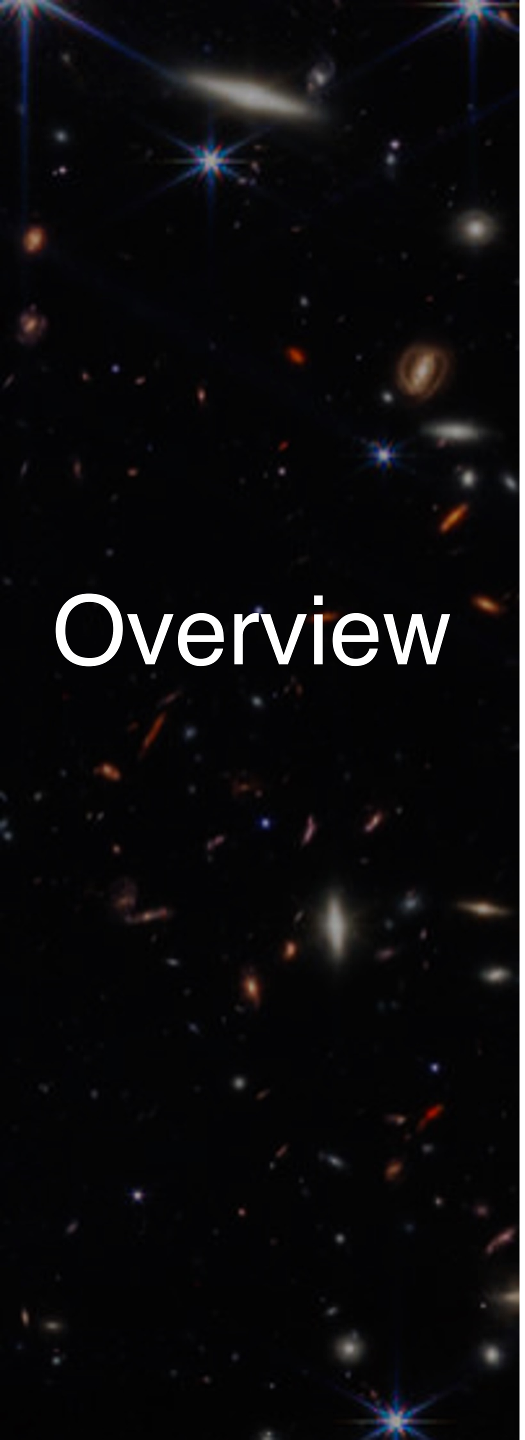

Overview

- Motivation
- Substructure in strong lensing
- Neural likelihood-ratio estimation
- Modeling details & results
- Summary

Substructure as a probe of dark matter

- Alternative dark matter theories offer different predictions from CDM on sub-galactic scales
- Sub-galactic observables can be complicated by baryonic effects
- Low-mass subhalos ($<10^9 M_\odot$) are useful because of their lack of luminous matter

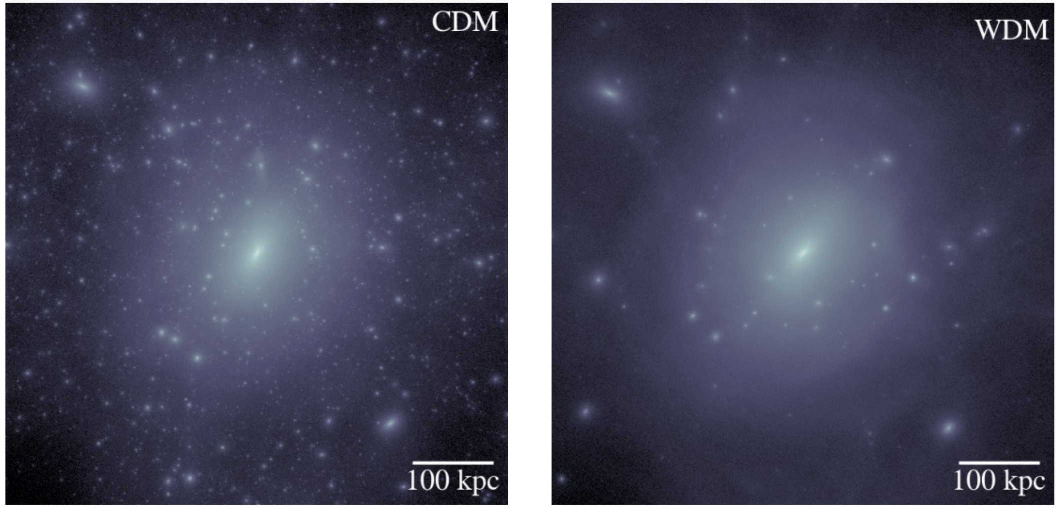

Bullock & Boylan-Kolchin, ARAA (1707.04256)

Strong gravitational lensing

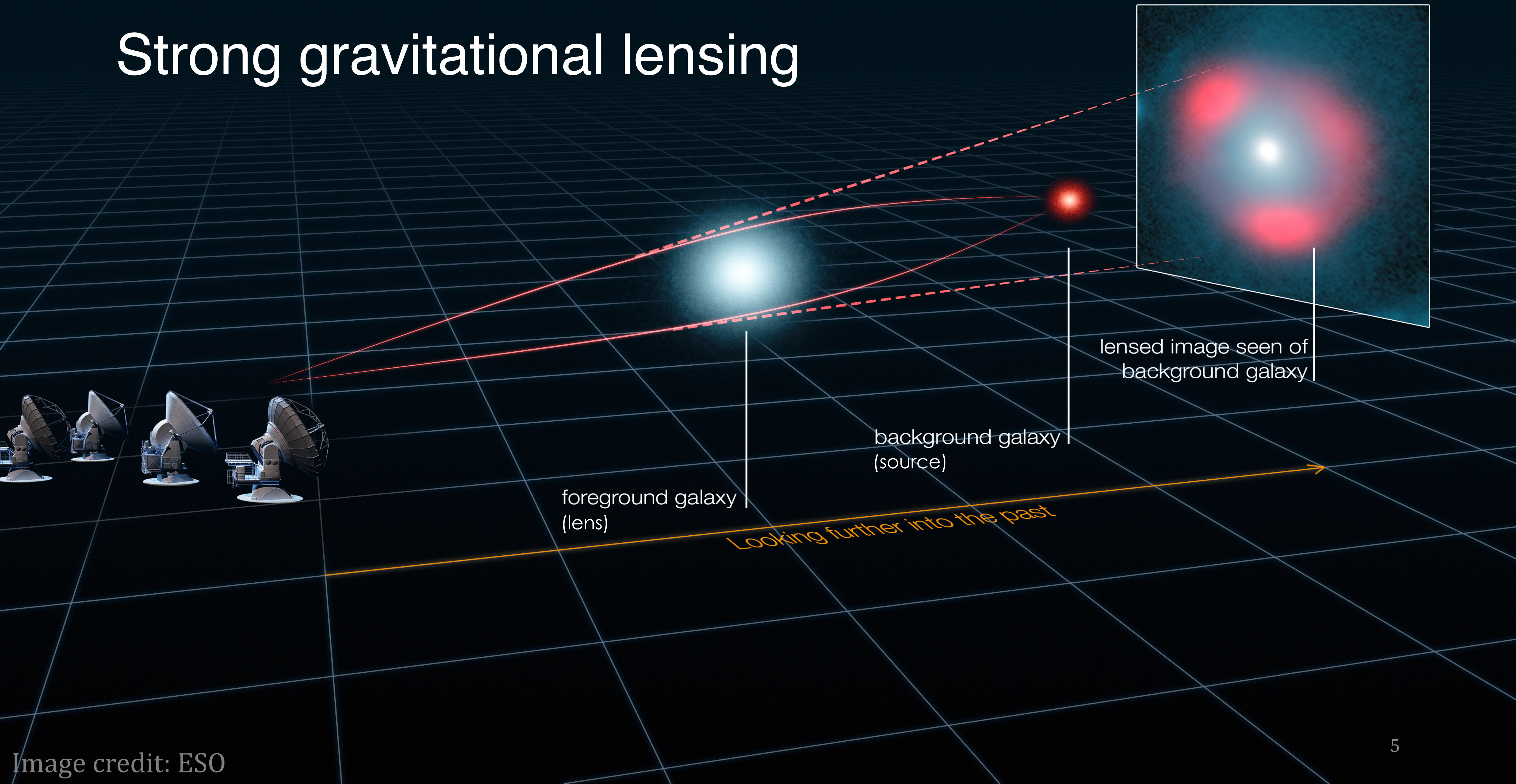

Image credit: ESO

How do we probe subhalos with strong lensing?

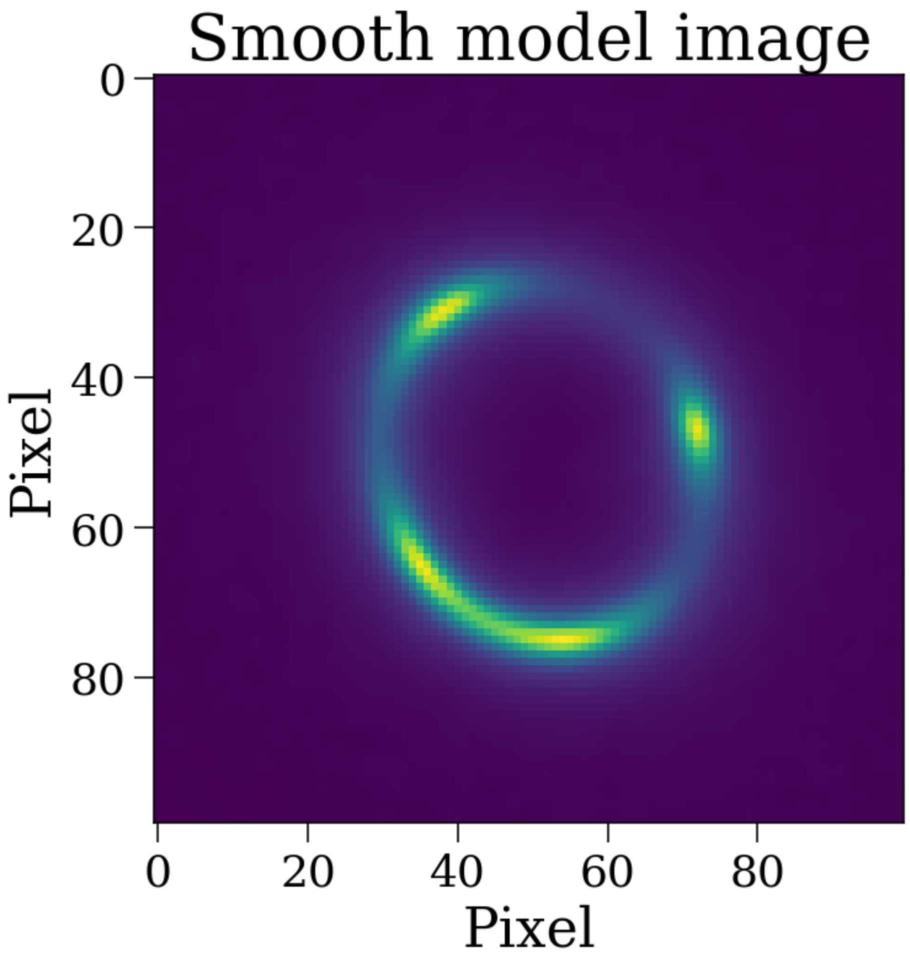

Pixel size = 0.04''

How do we probe subhalos with strong lensing?

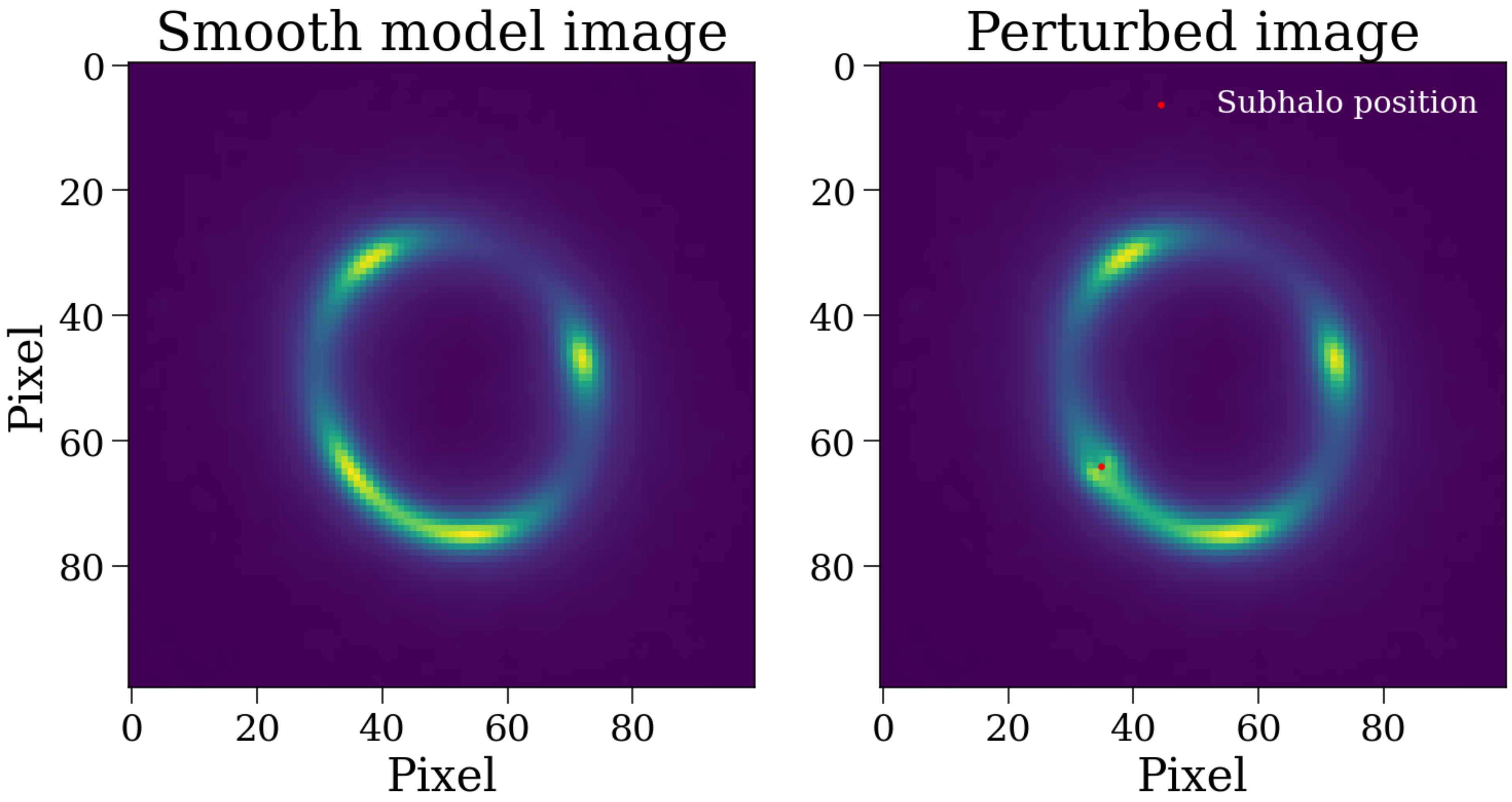

Pixel size = 0.04''

Subhalo effective density slope

- With finite image resolution, a subhalo can be approximated by a power-law 3D density profile $\rho(r) \propto r^{-\gamma}$

JVAS B1938+666 with HST data

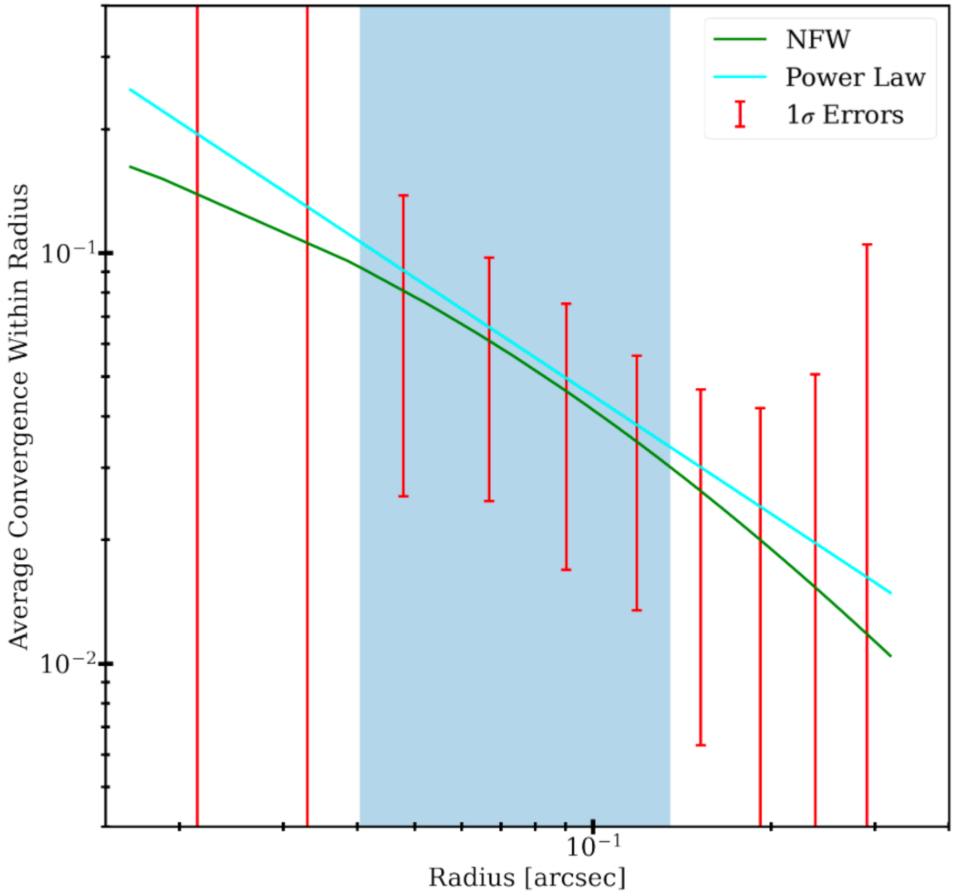

Şengül & Dvorkin, MNRAS (2206.10635)

Subhalo effective density slope

- With finite image resolution, a subhalo can be approximated by a power-law 3D density profile $\rho(r) \propto r^{-\gamma}$

JVAS B1938+666 with HST data

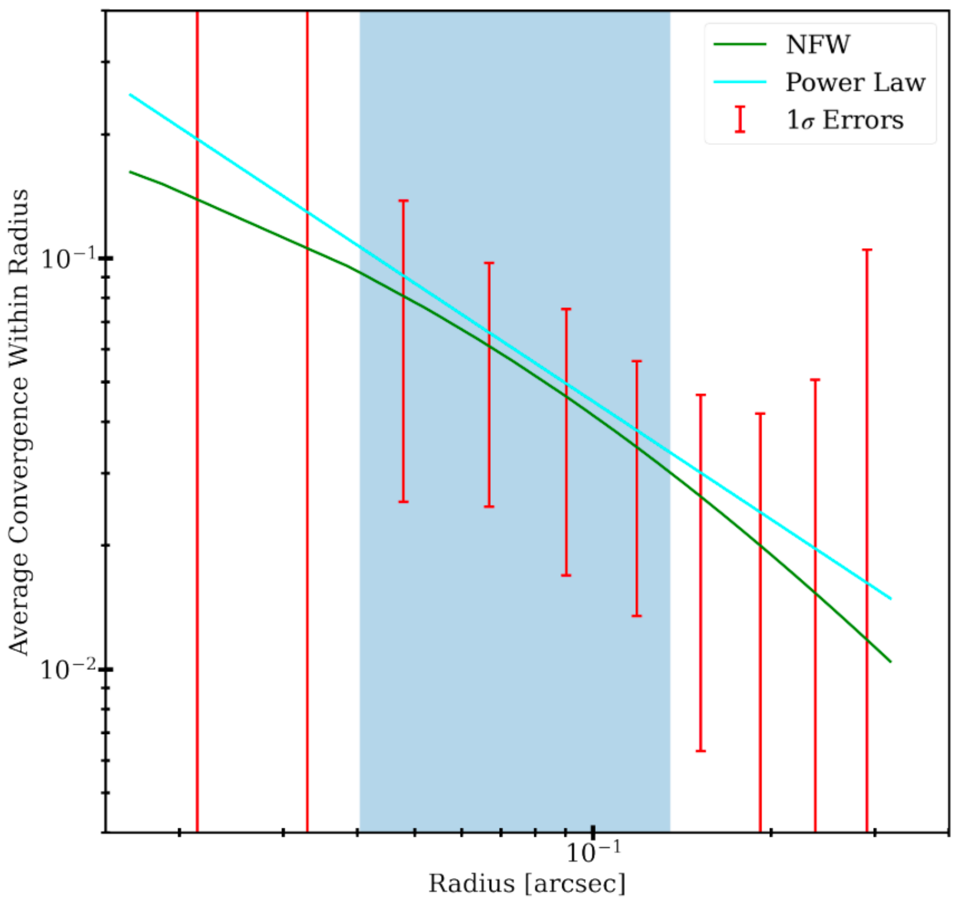

Şengül & Dvorkin, MNRAS (2206.10635)

Subhalo effective density slope

- With finite image resolution, a subhalo can be approximated by a power-law 3D density profile $\rho(r) \propto r^{-\gamma}$
- Individually constraining density slopes is computationally expensive and restrictive

JVAS B1938+666 with HST data

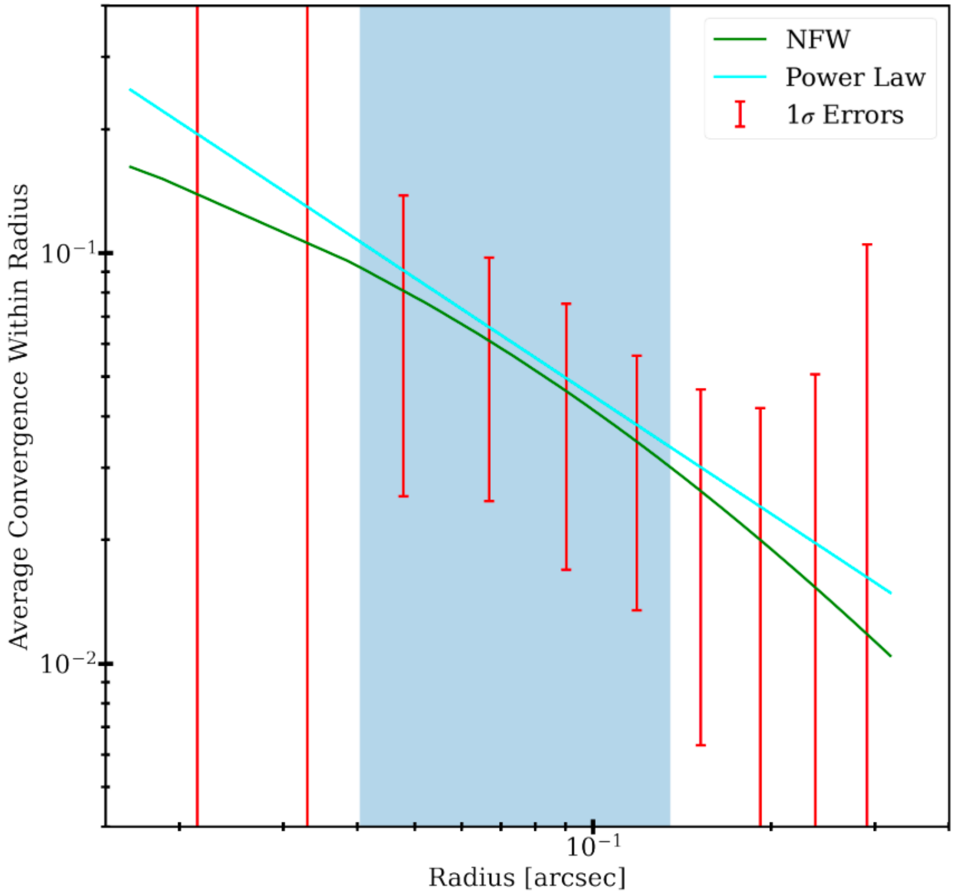

Şengül & Dvorkin, MNRAS (2206.10635)

Likelihood-ratio estimation

$$\begin{tikzcd}
 & & p(\gamma, x) \arrow[dr] & \\
\gamma \arrow[r] & \{\gamma, x\} \arrow[ur] \arrow[dr] & & r(x|\gamma) = \dfrac{p(\gamma, x)}{p(\gamma)p(x)} \arrow[d, leftrightarrow] \\
 & & p(\gamma)p(x) \arrow[ur] & s(\gamma, x) = \dfrac{p(\gamma, x)}{p(\gamma, x) + p(\gamma)p(x)}
\end{tikzcd}$$

Cranmer et al., 2015 (1506.02169)
Hermans et al., 2019 (1903.04057)

Likelihood-ratio estimation

$$
\begin{tikzcd}
 & & p(\gamma,x) \arrow[dr] & \\
\gamma \arrow[r] & \{\gamma,x\} \arrow[ur] \arrow[dr] & & r(x|\gamma) = \dfrac{p(\gamma,x)}{p(\gamma)p(x)} \arrow[d, leftrightarrow] \\
 & & p(\gamma)p(x) \arrow[ur] & s(\gamma,x) = \dfrac{p(\gamma,x)}{p(\gamma,x)+p(\gamma)p(x)}
\end{tikzcd}
$$

- The inferred likelihood-ratios of multiple observations with the same underlying γ can be easily combined

$$\hat{r}(\{x\}|\gamma) = \prod_i \hat{r}(x_i|\gamma)$$

Cranmer et al., 2015 (1506.02169)
Hermans et al., 2019 (1903.04057)

Likelihood-ratio estimation

$\gamma \longrightarrow \{\gamma, x\}$

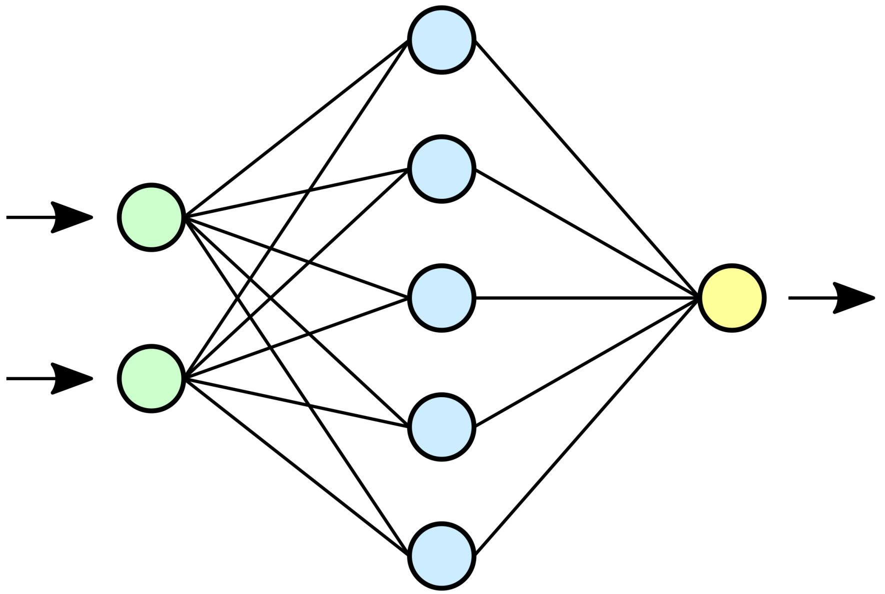

$$r(x|\gamma) = \frac{p(\gamma, x)}{p(\gamma)p(x)}$$

$$\updownarrow$$

$$s(\gamma, x) = \frac{p(\gamma, x)}{p(\gamma, x) + p(\gamma)p(x)}$$

- The inferred likelihood-ratios of multiple observations with the same underlying γ can be easily combined

$$\hat{r}(\{x\}|\gamma) = \prod_i \hat{r}(x_i|\gamma)$$

Cranmer et al., 2015 (1506.02169)
Hermans et al., 2019 (1903.04057)

Mock data modeling

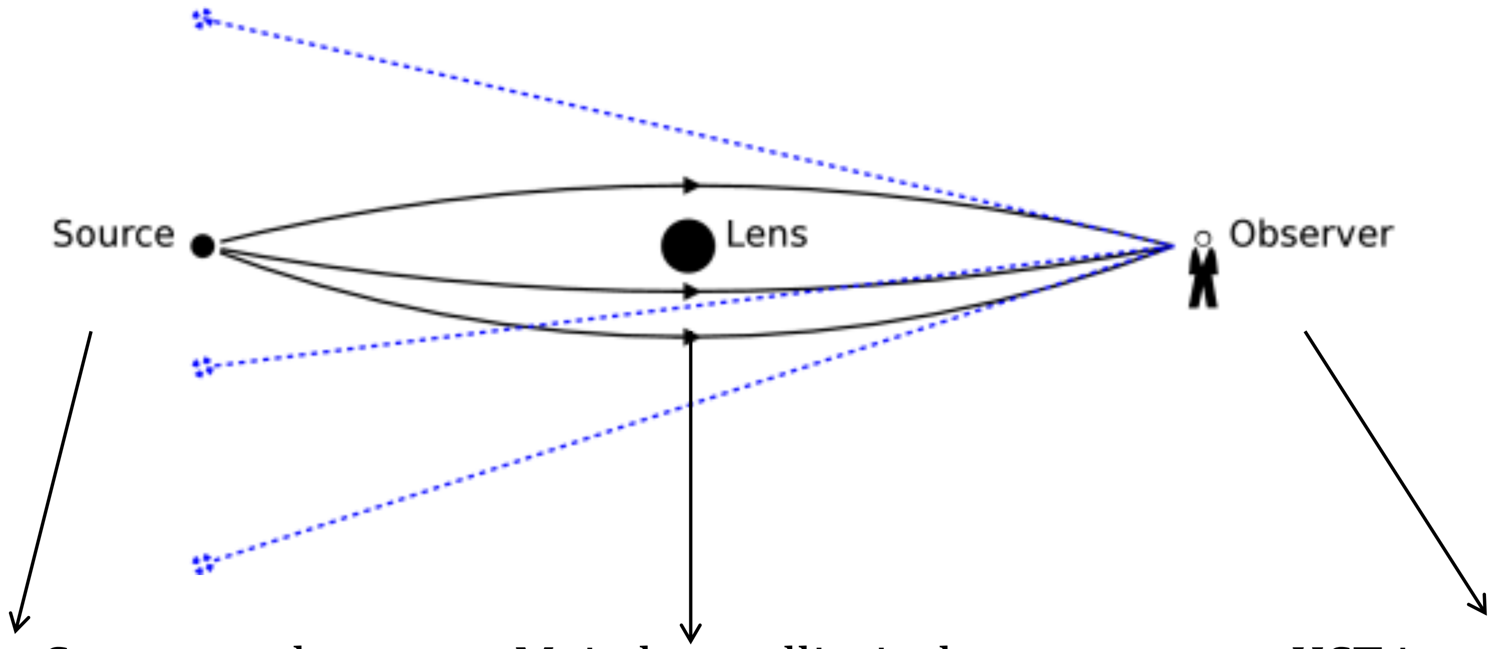

- PALTAS (Wagner-Carena et al., ApJ, 2023)
- Hubble Space Telescope (HST) COSMOS survey galaxies

- Main lens: elliptical power-law (EPL) with shear, multipole moments, lens light
- Subhalos & LoS halos (next slide)

- HST instrumentation effects (empirical PSF, noise, etc.)

Lenstronomy (Birrer et al., ApJ, 2015)

Mock data modeling

Subhalos & LoS halos

- Training and validation set (EPL): $\rho(r) \propto r^{-\gamma}$
- Test set (NFW and truncated NFW):

$$\rho(r) = \frac{\rho_0}{\frac{r}{r_s}\left(1+\frac{r}{r_s}\right)^2}$$

This can be also parametrized by concentration c_{200} and mass M_{200} where $r_{200} = c_{200} r_s$

- Simulate different effective density slopes by changing the CDM mass-concentration relation

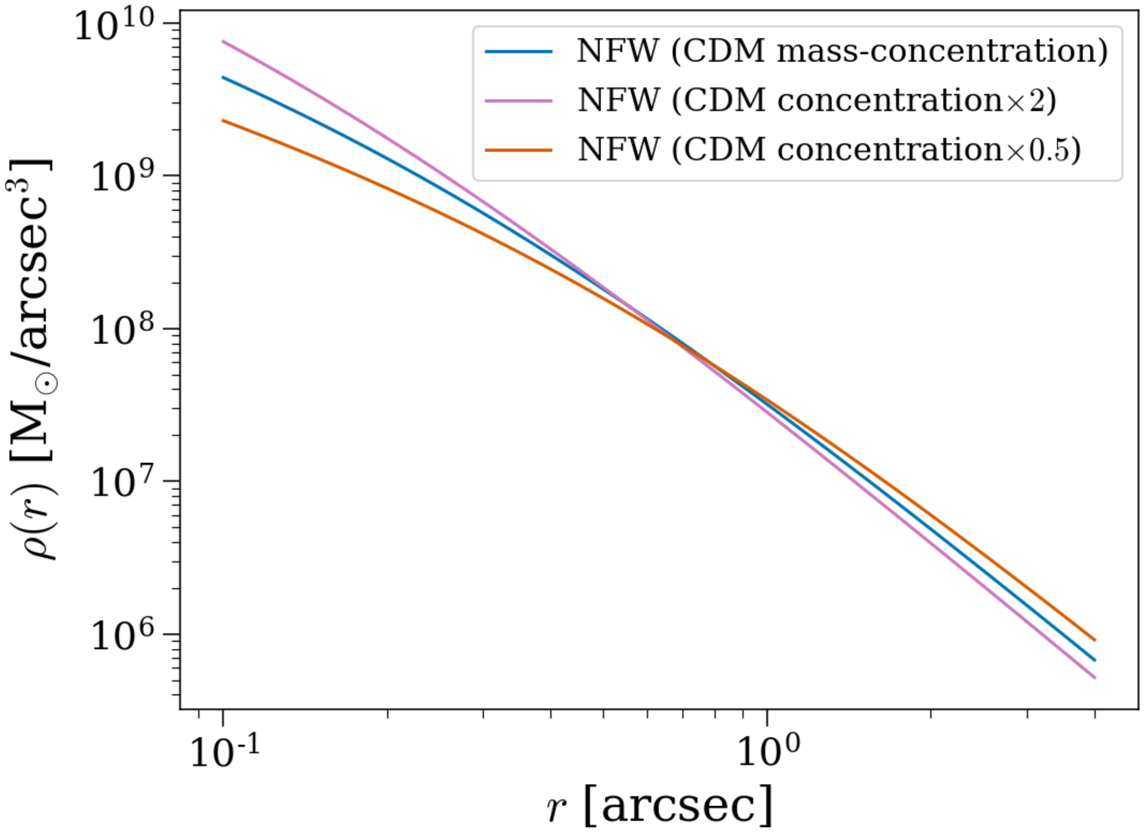

Neural network details

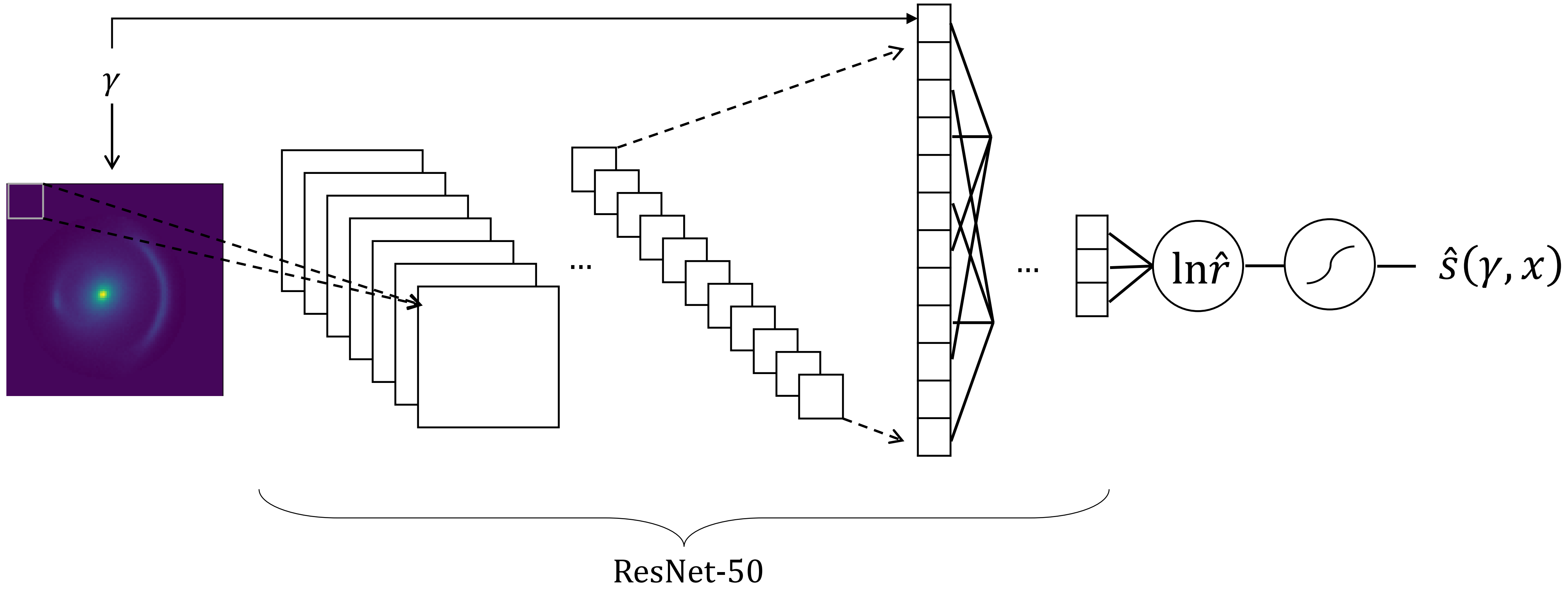

Neural network details

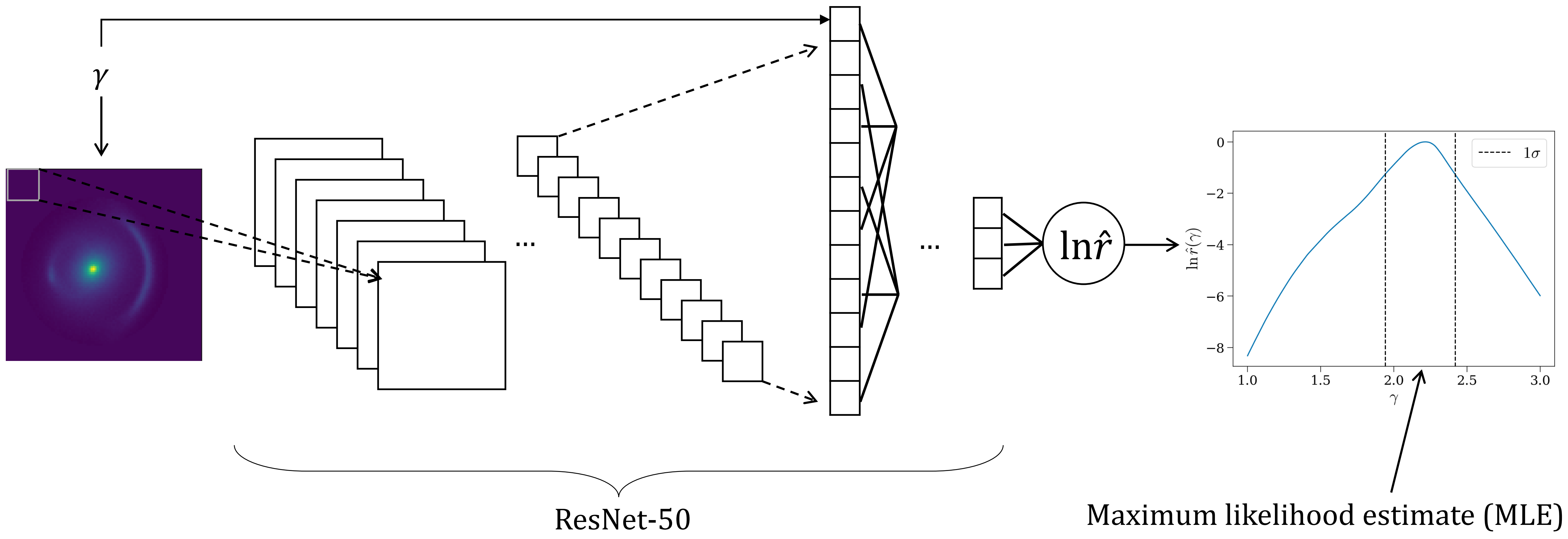

Model evaluation

Individual images with power-law substructure

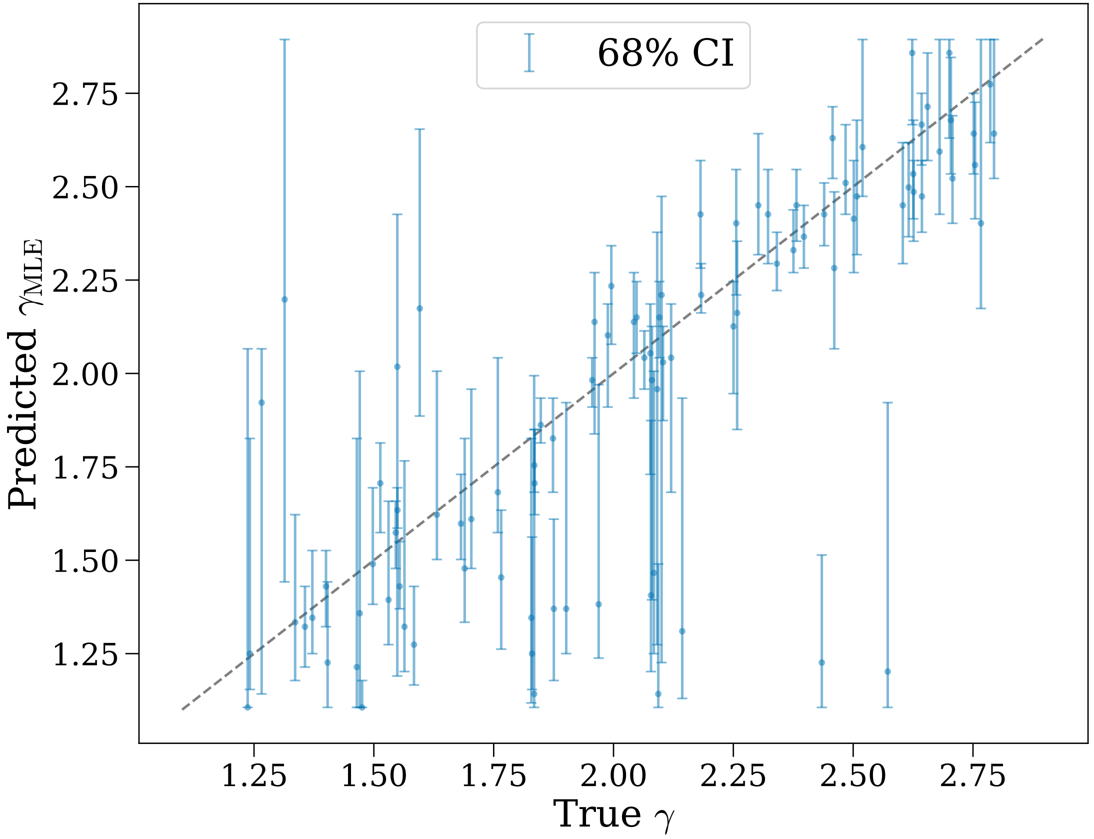

Sets of 13 images with power-law substructure

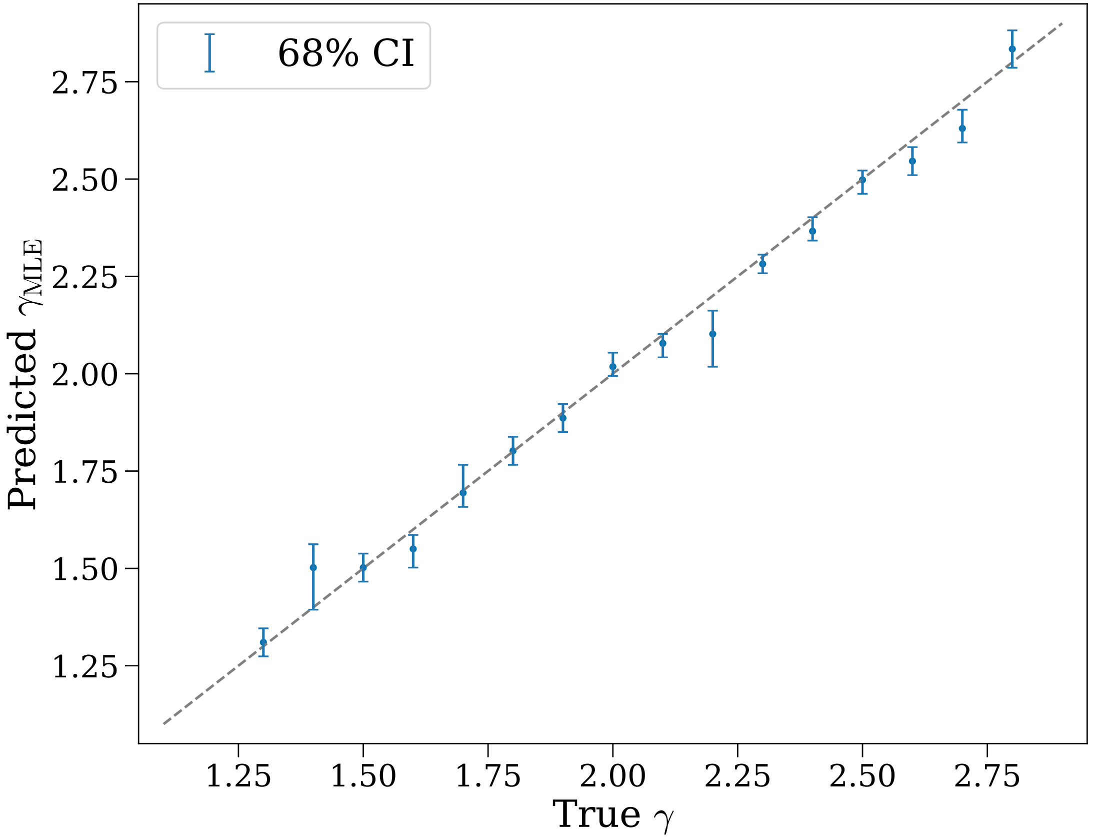

Results

Sets of 13 images with (t)NFW substructure

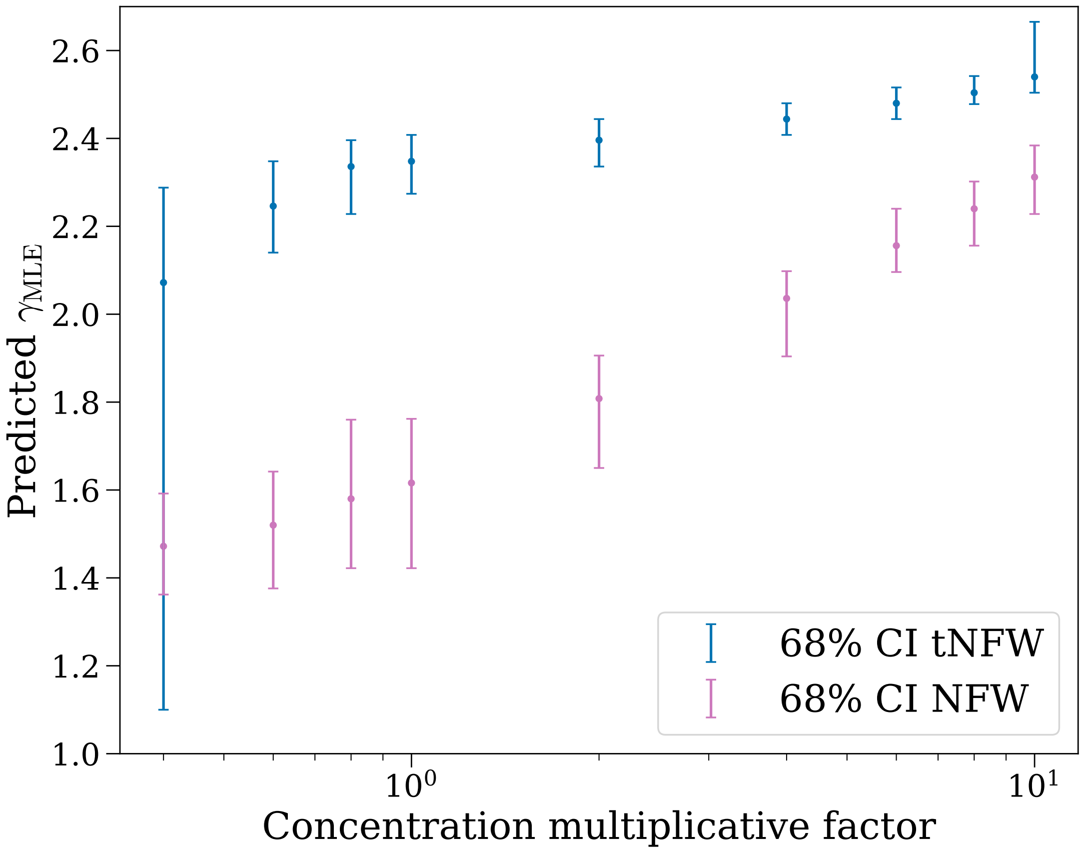

Theoretical predictions vs. HST measurement

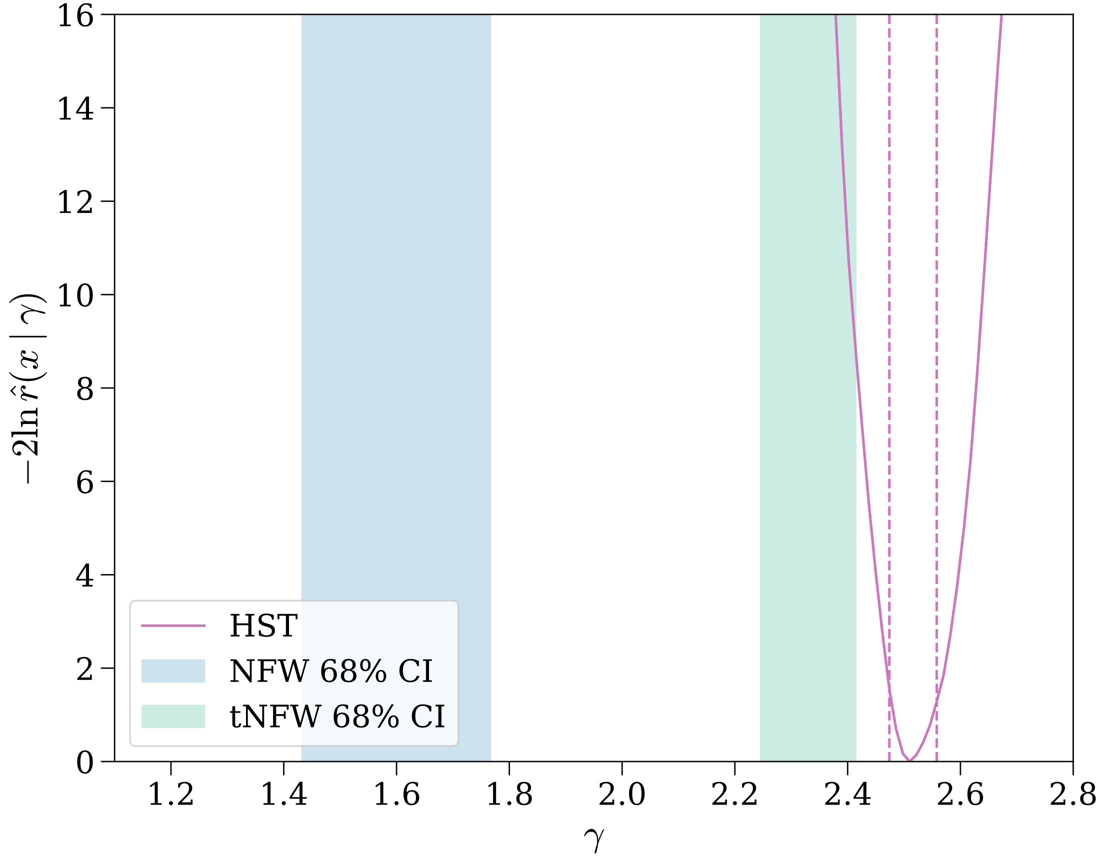

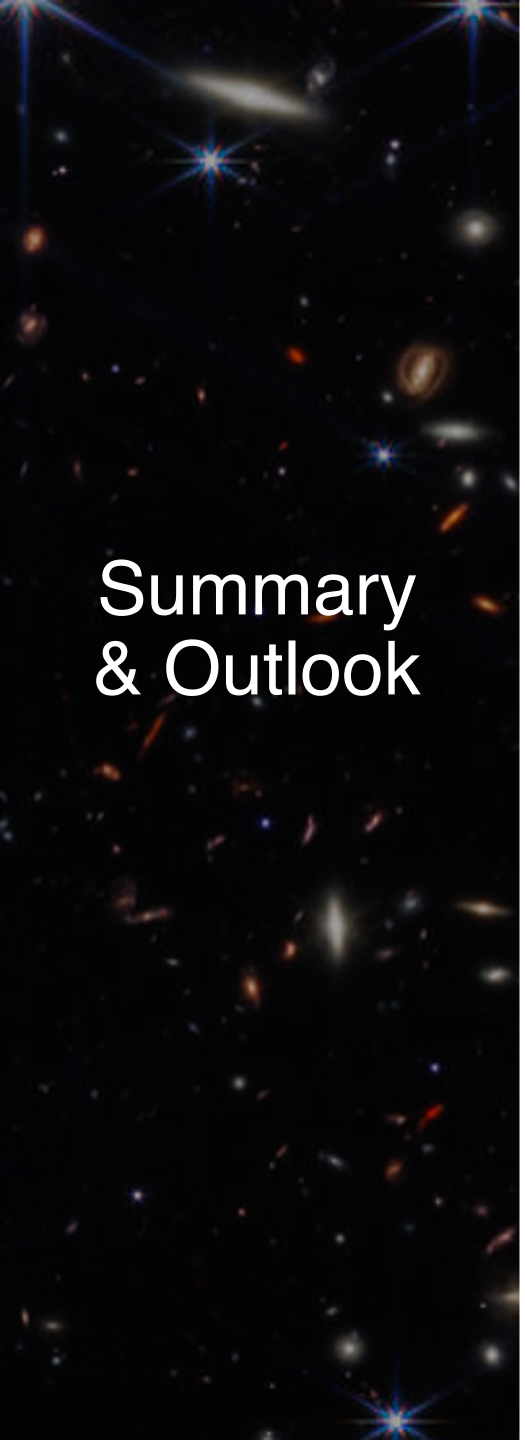

Summary & Outlook

- Neural likelihood-ratio estimation is effective and efficient at probing differences in substructure density slopes

- More remains to be done: predictions under different microphysical DM models, examining selection effects, etc.

Image credit: NASA

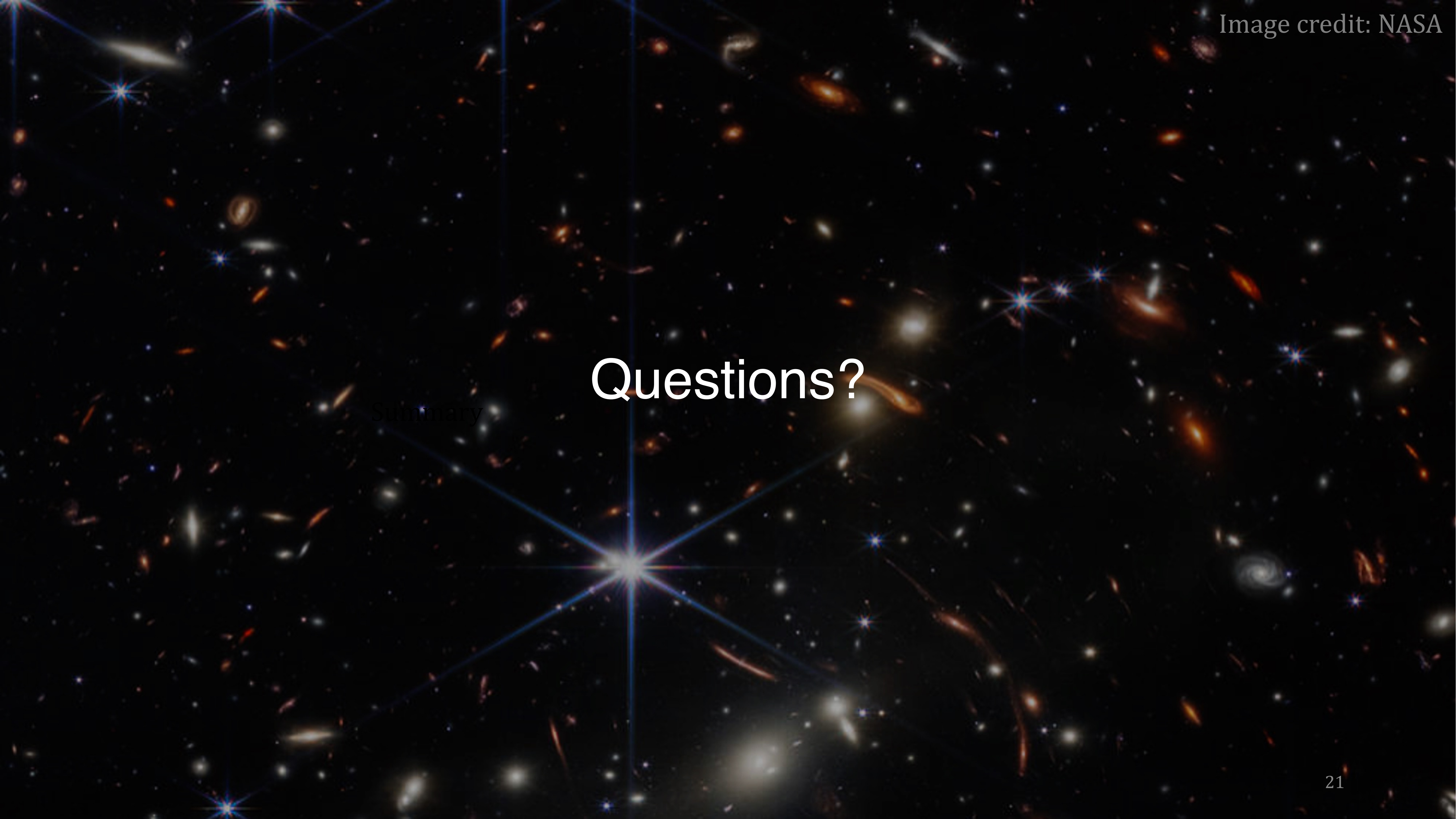

Questions?

Summary

Backup slides

Parameter	Distribution
Source	
Source redshift	$z_{\mathrm{source}} \sim \mathcal{U}(0.5, 0.7)$
x-coordinate	$x_{\mathrm{source}} \sim \mathcal{U}(-0.1'', 0.1'')$
y-coordinate	$y_{\mathrm{source}} \sim \mathcal{U}(-0.1'', 0.1'')$
Main lens	
Lens redshift	$z_{\mathrm{lens}} \sim \mathcal{U}(0.15, 0.25)$
x-coordinate	$x_{\mathrm{lens}} \sim \mathcal{U}(-0.2'', 0.2'')$
y-coordinate	$y_{\mathrm{lens}} \sim \mathcal{U}(-0.2'', 0.2'')$
Einstein radius	$\theta_E \sim \mathcal{U}(0.9'', 1.3'')$
Ellipticities	$e_1 \sim \mathcal{U}(-0.2, 0.2) \quad e_2 \sim \mathcal{U}(-0.2, 0.2)$
Multipole moments ($m = 3, 4$)	$a_m \sim \mathcal{U}(0, 0.05) \quad \phi_m \sim \mathcal{U}(-\pi, \pi)$
EPL slope of density profile	$\gamma_{\mathrm{ML}} \sim \mathcal{N}(2, 0.1)$
External shear	$\gamma_{\mathrm{shear},1} \sim \mathcal{U}(-0.1, 0.1) \quad \gamma_{\mathrm{shear},2} \sim \mathcal{U}(-0.1, 0.1)$
Lens light	
Apparent magnitude	$m \sim \mathcal{U}(17, 19)$
Half light radius	$R_{\mathrm{sersic}} \sim \mathcal{N}(0.8, 0.15)$
Sérsic index	$n_{\mathrm{sersic}} \sim \mathcal{N}(2, 0.5)$
Ellipticities	$e_1 \sim \mathcal{U}(-0.1, 0.1) \quad e_2 \sim \mathcal{U}(-0.1, 0.1)$
LoS halos	
EPL ellipticities	$e_1 \sim \mathcal{U}(-0.2, 0.2) \quad e_2 \sim \mathcal{U}(-0.2, 0.2)$
EPL slope of density profile per lens system	$\gamma \sim \mathcal{U}(1.1, 2.9)$
EPL slope of density profile per subhalo	$\gamma_i \sim \mathcal{N}(\gamma, 0.1\gamma)$
LoS halo mass	$M_{200} \in [10^7, 10^{10}]\mathrm{M}_\odot$
Halo mass function normalization	$\delta_{\mathrm{los}} \sim \mathcal{U}(0, 2)$
Subhalos	
EPL ellipticities	$e_1 \sim \mathcal{U}(-0.2, 0.2) \quad e_2 \sim \mathcal{U}(-0.2, 0.2)$
EPL slope of density profile per lens system	$\gamma \sim \mathcal{U}(1.1, 2.9)$
EPL slope of density profile per subhalo	$\gamma_i \sim \mathcal{N}(\gamma, 0.1\gamma)$
Subhalo mass function power-law slope	-1.9
Subhalo mass	$M_{200} \in [10^7, 10^{10}]\mathrm{M}_\odot$

Training details

- Training data preprocessing: zero mean and unit standard deviation on images and zero mean on slopes
- Loss: BCE
- Optimizer: AdamW
- Batch size: 2000 (small size affects training stability)

Set of HST images analyzed

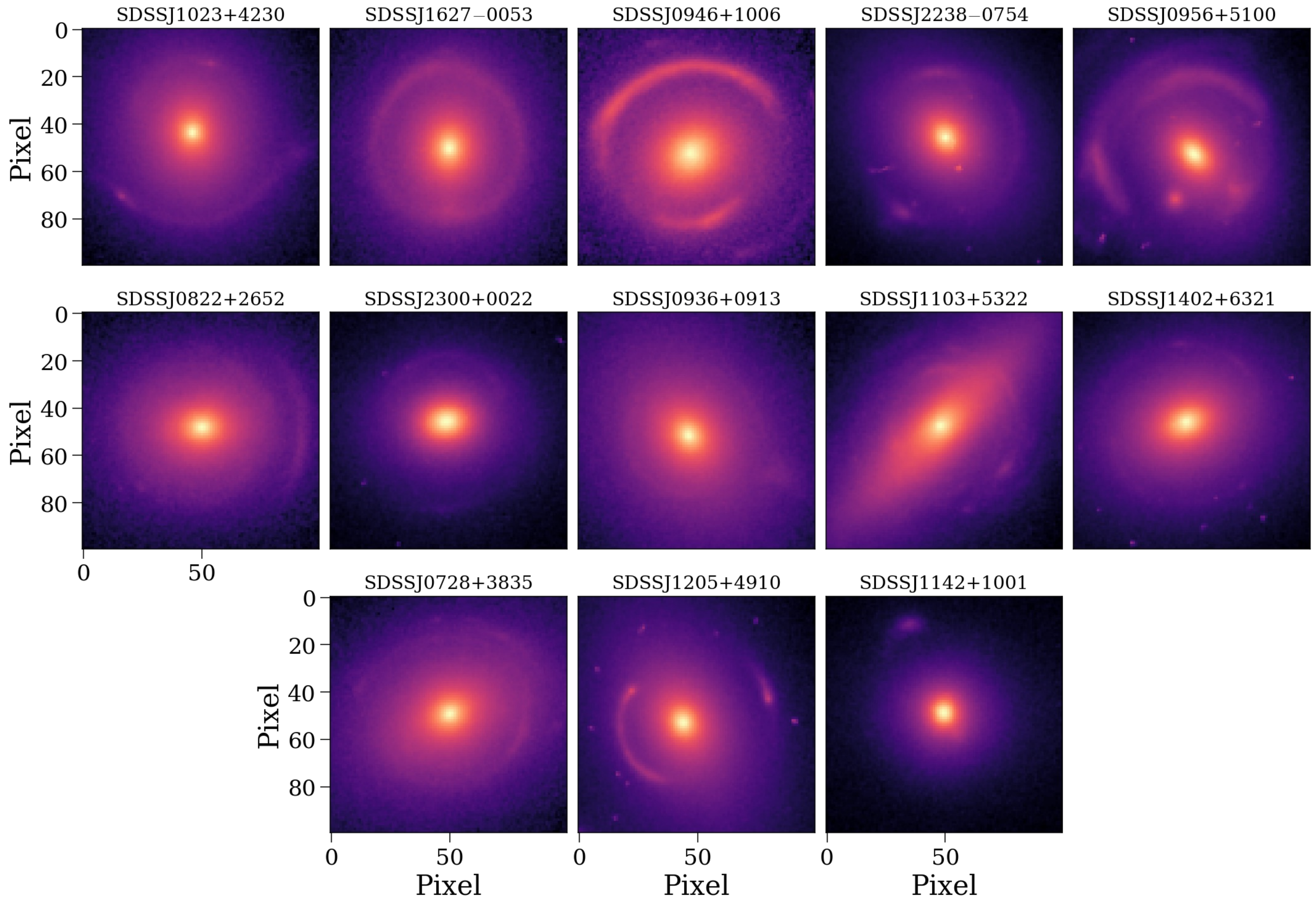

Sample likelihood ratios of HST images

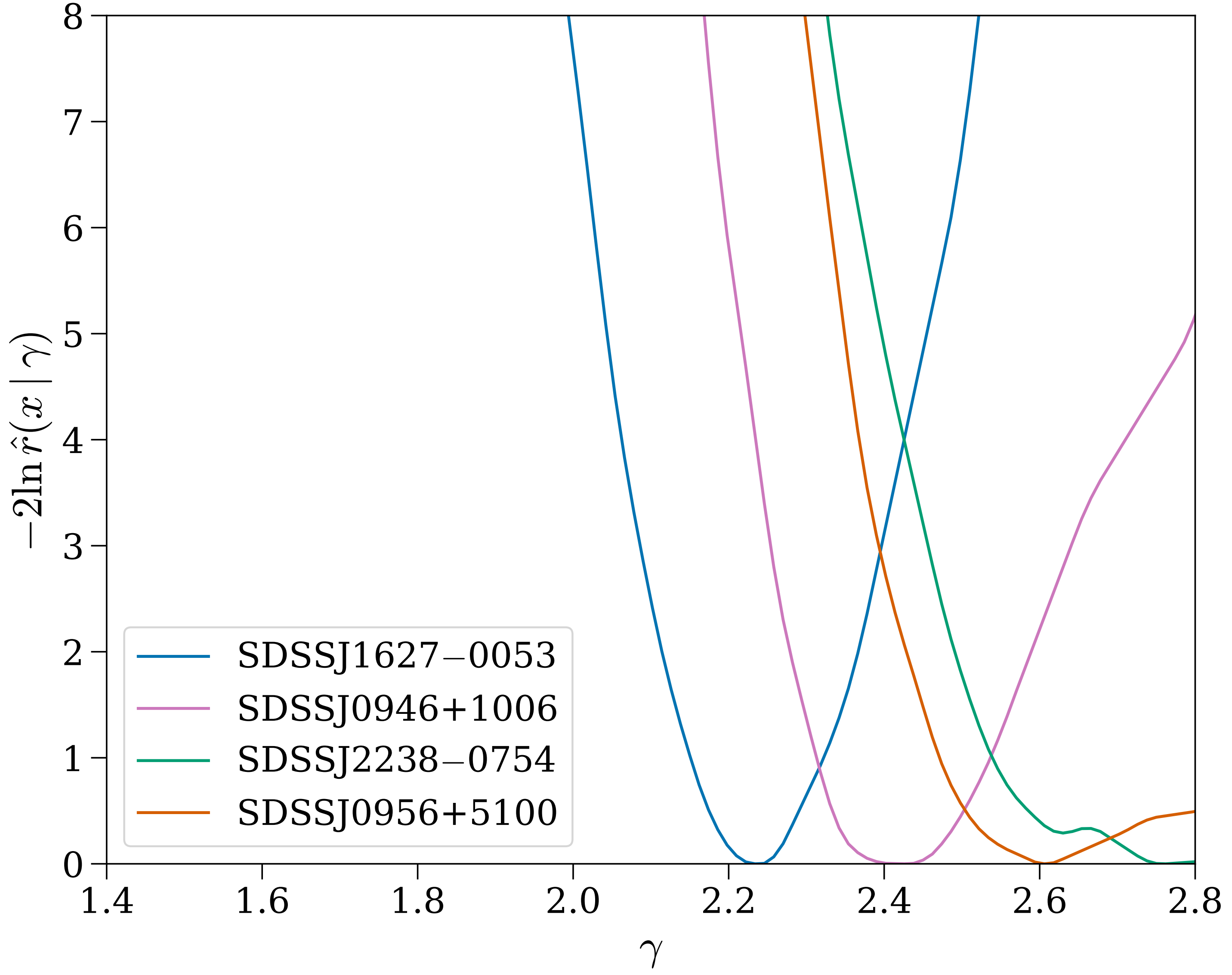

Mass-concentration relation

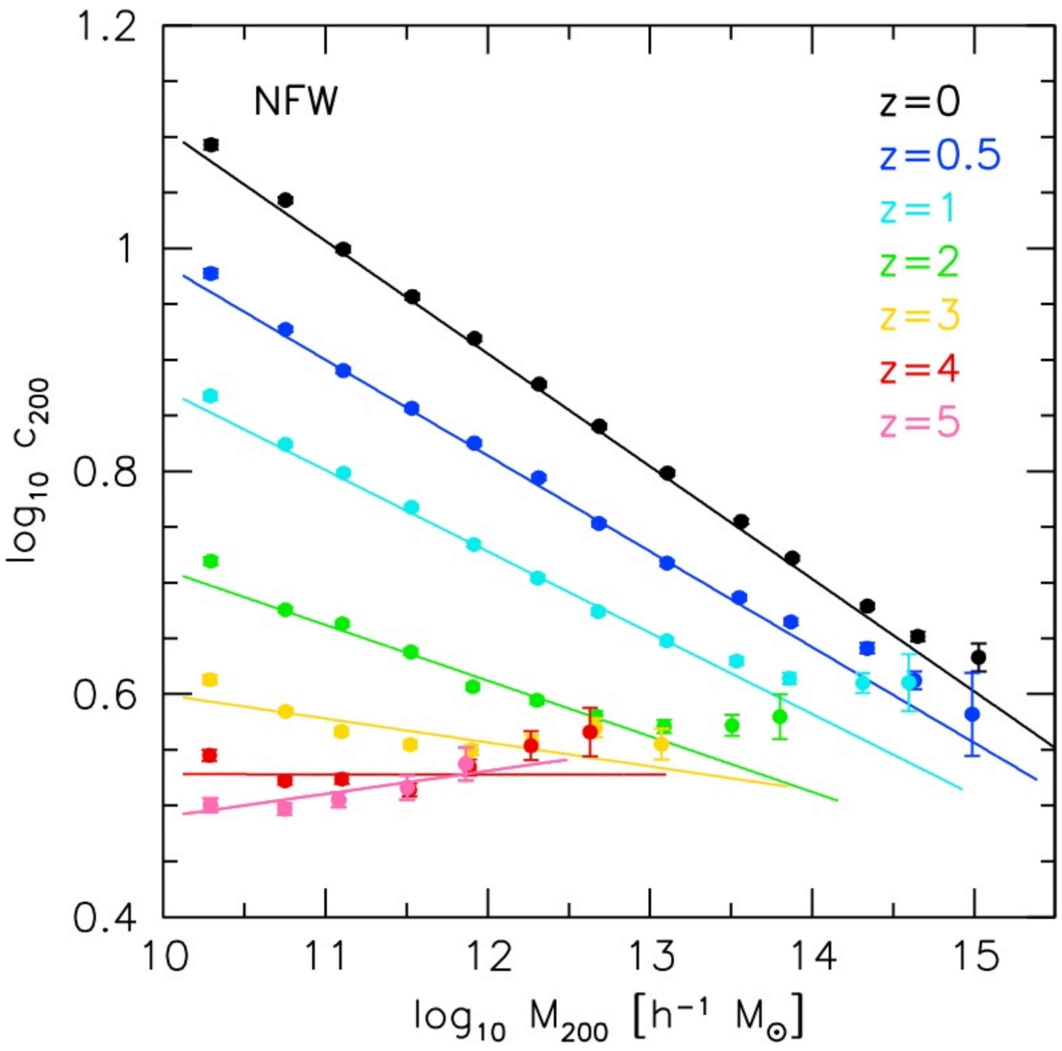

Table 3. Fit parameters for the concentration mass relation: $\log_{10} c = a + b \log_{10}(M/[10^{12} h^{-1} \mathrm{M}_\odot])$.

Profile	Δ	Redshift	zero point (a)	slope (b)
NFW	200	0.0	0.905 ±0.001	-0.101 ±0.001
NFW	200	0.5	0.814 ±0.001	-0.086 ±0.001
NFW	200	1.0	0.728 ±0.001	-0.073 ±0.001
NFW	200	2.0	0.612 ±0.001	-0.050 ±0.001
NFW	200	3.0	0.557 ±0.003	-0.021 ±0.002
NFW	200	4.0	0.528 ±0.004	0.000 ±0.003
NFW	200	5.0	0.539 ±0.006	0.027 ±0.005

Dutton & Macciò, 2014, MNRAS

RMO comparison

$M_{200} \approx 1.5{\times}10^7 \mathrm{M}_\odot$
$\gamma \approx 2.55$

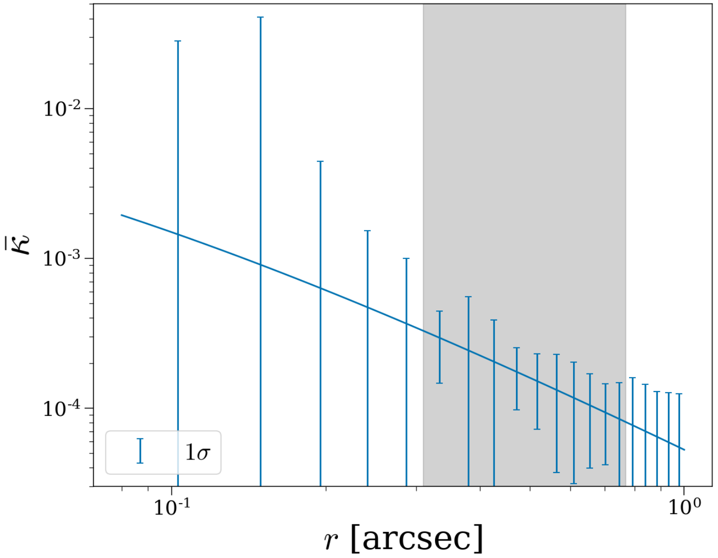

$M_{200} \approx 1.6{\times}10^9 \mathrm{M}_\odot$
$\gamma \approx 2.13$

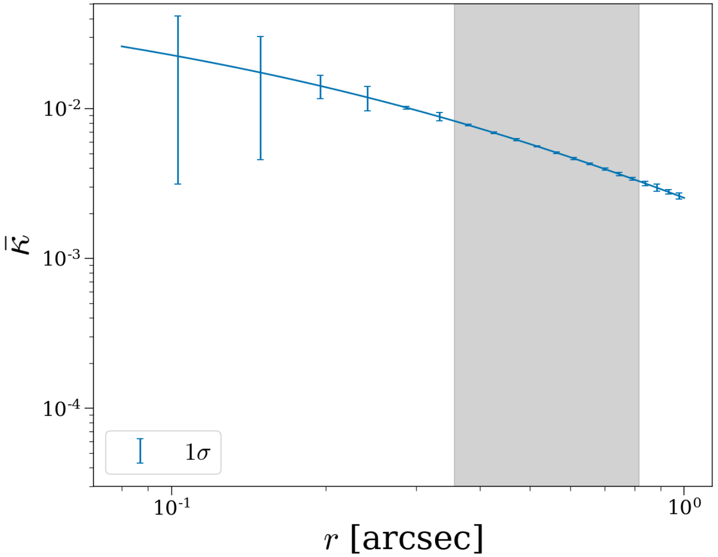

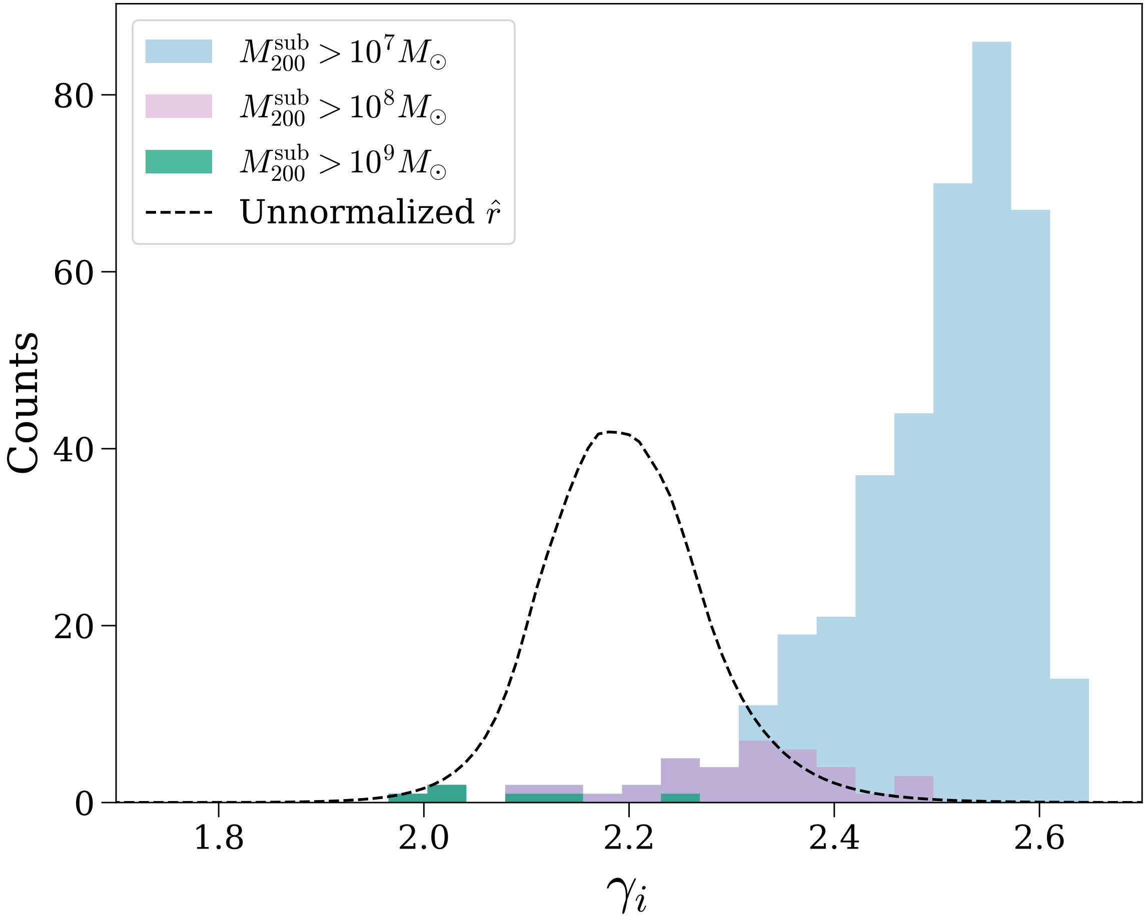

Sensitivity to subhalo population